Int. J. Solids Structures Vol. 23, No 5, pp. 607–619, 1987
Printed in Great Britain.

0020-7683/87 $3.00+.00

DISLOCATION–CRACK EDGE INTERACTION IN DYNAMIC BRITTLE FRACTURE AND CRACK PROPAGATION

L. M. BROCK
Engineering Mechanics, University of Kentucky, Lexington, KY 40506, U.S.A.

and

M. JOLLES
Code 6382, Naval Research Laboratory, Washington, DC, 20375, U.S.A.

(*Received* 27 *March* 1986)

Abstract—Due to the formation of small inelastic zones near crack edges, brittle fracture and crack propagation involve dislocation–crack edge interaction. An approximate transient solution for a single screw dislocation moving near a propagating Mode III crack is obtained here, and used to study dislocation arrays which exist prior to fracture in circular zones around the crack edge. Using dislocation force concepts, it is found that these dislocations coalesce into bands near the crack surface when fracture is triggered by SH-wave diffraction and, if their speeds exceed that of the crack edge, collapse onto the crack surface itself. Moreover, this dislocation motion has a noticeable if brief effect on the dynamic stress intensity factor.

1. INTRODUCTION

Brittle fracture is often associated with the formation of small inelastic zones at the crack edges[1]. Because inelastic regions are characterized by dislocation fields[2], it follows that brittle fracture itself must involve a process of dislocation–crack edge interaction[3].

Much of the existing analysis of such interaction is quasi-static, e.g. Refs [4–6], with little application, therefore, to dynamic brittle fracture. Transient analyses of largely arbitrary screw dislocation motion near a crack edge do exist[7–9], but the cracks considered are stationary, thus limiting insight into crack propagation.

This article, therefore, performs two tasks in a preliminary study of dislocation–crack edge interaction in dynamic brittle fracture and crack propagation: first, it presents an approximate solution for the basic problem of largely arbitrary screw dislocation motion near a propagating semi-infinite Mode III crack. The crack and dislocation exist initially in equilibrium in an unbounded, isotropic, homogeneous, linearly elastic plane. The dislocation begins to move after it receives the first signal that the crack has started to propagate. This assumption is made only for illustration; the solution technique itself is rather general.

Then, this article applies the basic problem solution to the case of a screw dislocation array surrounding a crack subjected to SH-wave diffraction. Dislocation force concepts are used to prescribe the dislocation motions. The dynamic stress intensity factor and the dislocation trajectories are then studied in view of crack and dislocation speeds. The basic problem is formulated in the next section, and then solved by a superposition-based scheme which allows the use of much previous analysis.

2. BASIC PROBLEM FORMULATION

Consider the unbounded plane in Fig. 1(a) containing a crack defined by the Cartesian coordinates (x_1, x_2) as $x_2 = 0, x_1 < 0$. For $s < 0$, where s = (rotational wave speed) × (time), the crack is in equilibrium with a single screw dislocation of Burger's vector magnitude b. As shown in Fig. 1(a), the polar coordinates of the dislocation with respect to the crack edge are (d, ψ). For $s > 0$, the crack propagates in Mode III along the positive x_1-axis so that the instantaneous position of its edge is $x_2 = 0, x_1 = C(s)$. The function C is continuous,

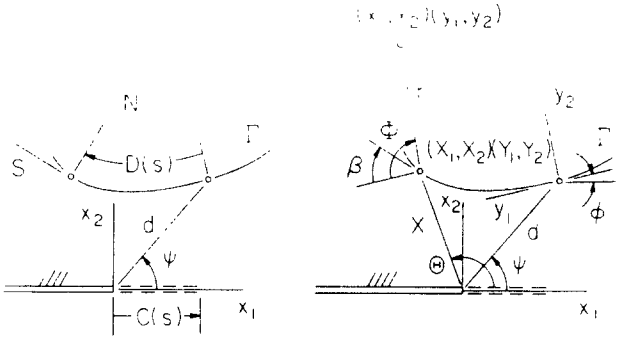

Fig. 1. (a) Dislocation–crack edge geometry. (b) Dislocation–crack edge parameters.

single-valued, and exhibits the properties $C(0) = 0$ and $0 \leqslant C < 1$, $s \geqslant 0$, where $(\cdot)$ denotes s-differentiation. These properties guarantee that the crack edge does not retreat along the x_1-axis and, in view of the definition of s, that it does not reach the rotational wave speed.

The propagating crack radiates a cylindrical rotational wave which reaches the dislocation position at $s = d$. At $s = s_0 \geqslant d$, the dislocation begins to move along the continuous, piecewise smooth trajectory Γ shown in Fig. 1(a). In terms of the path-variable coordinates (S, N), the dislocation edge for $s > s_0$ can then be defined as $N = 0$, $S = D(s)$. The function D is continuous, single-valued, and exhibits the properties $D(s_0) = 0$ and $0 \leqslant D < 1$, $s > s_0$.

The equations governing this process for $s > 0$ are

$$\nabla^2 w + \frac{b}{\mu}\delta'(N)H(D - S) - \ddot{w} = 0, \qquad w(\mathbf{x}, 0^+) = w^0(\mathbf{x}) \tag{1a,b}$$

for all $\mathbf{x}$ except $x_2 = 0$, $x_1 < C$, where

$$T_2 = 0. \tag{2}$$

Here $w(\mathbf{x}, s)$ and $w^0(\mathbf{x})$ are the out-of-plane displacements for $s > 0$ and $s < 0$, $\mathbf{x} = (x_1, x_2)$ is the position vector of points in the plane, and T_k are tractions defined by

$$T_k = \mu \frac{\partial w}{\partial x_k} \qquad (k = 1, 2). \tag{3}$$

The parameter μ is the shear modulus, ∇^2 is the Laplacian operator, and the non-homogeneous term in eqn (1a) is the Burridge–Knopoff[10] dislocation body-force equivalent, where δ and H are the Dirac and Heaviside functions, and $(\,)'$ denotes differentiation with respect to the argument. In addition, we require that w satisfy appropriate radiation conditions.

3. FORMAL SOLUTION OF BASIC PROBLEM BY SUPERPOSITION

Consider now the function $w_b(\mathbf{x}, s)$ which satisfies everywhere in $\mathbf{x}$ the equations

$$\nabla^2 w_b + \frac{b}{\mu}\delta'(N)H(D - S)H(S) - \ddot{w}_b = 0, \qquad w_b(\mathbf{x}, 0^+) \equiv 0 \tag{4}$$

for $s > s_0$. Then, consider the functions $w_c(\mathbf{x}, s)$ and $\mathbf{w}_c^0(x, s)$ which for $s > 0$ are both defined by

$$\nabla^2 w - \ddot{w} = 0, \qquad w(\mathbf{x}, 0^+) \equiv 0 \tag{5}$$

everywhere in $\mathbf{x}$ except $x_2 = 0$, $x_1 < C$ and $x_2 = 0$, $0 < x_1 < C$ where, respectively

$$T_{2c} = -T_{2b}, \qquad T_{2c}^0 = -T_2^0. \tag{6a, b}$$

In addition, these functions satisfy appropriate radiation conditions. By superposition it is clear that the combination $w_b + w_c + w_c^0 + w^0$ satisfies eqns (1)–(3) for w.

Equations (4) show that w_b is the solution for the transient problem of a dislocation which appears instantaneously when $s = s_0$ at the point $(S, N) = 0$ in a crack-free plane and then moves along the trajectory Γ. This problem has been treated in Ref. [11] for the case $s_0 = 0$. Thus, by a simple argument shift, it can be shown that

$$2\pi w_b = b \int_{s_0}^{t^*} \frac{1}{r} \frac{\mathrm{d}r}{\mathrm{d}N} \frac{\dot{D}\tau}{\sqrt{(\tau^2 - r^2)}} \mathrm{d}t, \qquad \tau = s - t, \qquad r = |\mathbf{x} - \mathbf{X}| \tag{7a, c}$$

where the position vector $\mathbf{X} = (X_1, X_2)$ locates points $S = D(t)$ on Γ. The parameter t^* is defined by

$$t^* = s - r[D(t^*)] \tag{8}$$

under the restriction

$$1 + \dot{D}r'(D) \geqslant 0. \tag{9}$$

Relation (9) can be violated only if the dislocation nears ($r' < 0$) a point $\mathbf{x}$ at a speed which exceeds ($\dot{D} > 1$) the rotational wave speed, a possibility which has been precluded here.

The function w^0 is, of course, the equilibrium solution for the stationary crack and dislocation. It has been obtained in Ref. [5] by conformal mapping techniques as

$$2\pi w^0 = b \operatorname{Im} \ln \left(\frac{\sqrt{z} + \sqrt{d}\, \mathrm{e}^{\mathrm{i}\psi/2}}{\sqrt{z} - \sqrt{d}\, \mathrm{e}^{-\mathrm{i}\psi/2}} \right), \qquad z = x_1 + \mathrm{i}x_2. \tag{10}$$

With (w_b, w^0) in hand, the basic problem is reduced to finding the functions (w_c, w_c^0). This task is accomplished in Sections 4–7.

4. FORMAL SOLUTIONS FOR w_c, w_c^0

Standard Green's function methods readily lead to the formal solution

$$w = \frac{1}{\mu\pi} \iint_A T_2(u, t) \frac{\mathrm{d}u\, \mathrm{d}t}{\sqrt{[\tau^2 - (x_1 - u)^2 - x_2^2]}} \tag{11}$$

of eqn (5). Here (u, t) correspond to (x_1, s) and the integration area A is that portion of the u–t plane where both the argument of the radical is positive and T_2 is defined. From Ref.

[12] it can be shown that, for the case of w_c, T_{2c} for $x_2 = 0$ is given by eqn (6a) when $x_1 < C$, by the relation

$$T_{2c} = \frac{1}{\pi\sqrt{(\eta - K)}} \int_L^K T_{2b}\left(\frac{v - \xi}{\sqrt{2}}, \frac{v + \xi}{\sqrt{2}}\right) \frac{\sqrt{(K - v)}}{\eta - v} \mathrm{d}v \tag{12}$$

when $C < x_1 < s$, and vanishes otherwise. For the case of w_c^0, T_{2c}^0 for $x_2 = 0$ is given by eqn (6b) when $0 < x_1 < C$, by the relation

$$T_{2c}^0 = \frac{1}{\pi\sqrt{(\eta - K)}} \int_\xi^K T_2^0\left(\frac{v - \xi}{\sqrt{2}}, \frac{v + \xi}{\sqrt{2}}\right) \frac{\sqrt{(K - v)}}{\eta - v} \mathrm{d}v \tag{13}$$

when $C < x_1 < s$, and vanishes otherwise. In eqns (12) and (13) (ξ, η) are the characteristic variables

$$\sqrt{2}\xi = s - x_1, \qquad \sqrt{2}\eta = s + x_1 \tag{14}$$

and $\eta = K(\xi)$ defines the ξ–η plane trajectory of the crack edge. Therefore, K is the solution to

$$K - \xi = \sqrt{2}C\left(\frac{K + \xi}{\sqrt{2}}\right) \tag{15}$$

which follows from the substitution of eqn (14) into the relation $x_1 = C$. In eqn (12), $\eta = L(\xi)$ defines the ξ–η plane trajectory for the intersection of the stress wavefront radiating from the initial dislocation position $(S, N) = 0$ and the crack plane $x_2 = 0$. Therefore, L can be obtained from eqn (14) and Fig. 1(a) as

$$\sqrt{2}L = \frac{d^2 - s_0^2 + \sqrt{2}\xi(d_1 + s_0)}{\sqrt{2}\xi + d_1 - s_0}, \qquad d_1 = d\cos\psi, \qquad d_2 = d\sin\psi. \tag{16}$$

For purposes of studying solution behavior, the formal combinations of eqns (11)–(13) are, while exact, inconvenient. As a first step in getting these combinations into approximate but more tractable forms, eqn (12) is examined in the next section.

5. SIMPLIFICATION OF T_{2c}

In Fig. 1(b) we see that

$$r = |\mathbf{x} - \mathbf{X}| = |\mathbf{y} - \mathbf{Y}| \tag{17}$$

where $\mathbf{y} = (y_1, y_2)$ is the position vector in terms of a Cartesian coordinate system centered at the point $(S, N) = 0$ and aligned with the (S, N)-directions there, while $\mathbf{Y} = (Y_1, Y_2)$ locates points on the dislocation trajectory Γ. Upon substitution of eqn (17) into eqn (7a) in view of Fig. 1(b), it is easily shown that on Γ and for $x_2 = 0$, respectively

$$\frac{\mathrm{d}r}{\mathrm{d}N} = \sin(\beta - \Phi), \qquad \frac{\partial w_b}{\partial x_2} = -\frac{1}{x_1}\frac{\partial w_b}{\partial \phi} \tag{18a,b}$$

where ϕ is the slope angle of Γ at $(S, N) = 0$ with respect to the x_1-axis. Using these results along with eqn (8), and then substituting eqn (7a) into the right-hand side of eqn (12) along with the variable change $v = \xi - \sqrt{2}u$ yields the expression

$$T_{2c} = \frac{-\mu b}{2\pi^2\sqrt{(x_1 - C_1)}} \int_{s_0}^{t^*} \dot{D} \frac{\partial}{\partial \phi} \frac{1}{\sqrt{[2(B + X_1)]}} \int_{-C_1}^{U} \frac{B - u}{u^2 + X^2 + 2uX_1} \times \sqrt{\left(\frac{u + C_1}{U - u}\right)} \frac{F(u)}{x_1 + u} \mathrm{d}u\, \mathrm{d}t \tag{19}$$

for $C < x_1 < s$, where x_1 is small. In eqn (19)

$$B = s - x_1 - t, \qquad U = \frac{1}{2}\frac{B^2 - X^2}{B + X_1}, \qquad F(u) = \frac{X}{u}\sin(\phi - \beta - \Theta) + \sin(\phi - \beta)$$
$$C_1 = C(s_1), \qquad X = |\mathbf{X}| \tag{20}$$

where, as seen in Fig. 1(b), (X, Θ) are the polar coordinates of the trajectory points $\mathbf{X}$ with respect to the initial crack edge and β is the slope angle of the trajectory with respect to the y_1-axis. The instants (s_1, t^*) follow from the equations

$$s_1 - C_1 = s - x_1, \qquad t^* = s - x_1 + C_1 - r_1^* \tag{21}$$

where $(\,)^*$ denotes a quantity evaluated at $t = t^*$, $S = D(t^*)$, and (r_1, ω_1) defined by

$$X_1 - C_1 = r_1 \cos\omega_1, \qquad X_2 = r_1 \sin\omega_1 \tag{22}$$

are the polar coordinates of the trajectory points $\mathbf{X}$ at $S = D(t)$ with respect to the point $\mathbf{x} = (C_1, 0)$.

The u-integral in eqn (19) is along the integrand branch cut $-C_1 < u < U$, and the integrand itself exhibits simple poles at $u = -x_1 < 0$ and $u = -X_1 \pm \mathrm{i}|X_2|$, and as indicated by the Principal Value integration, a point singularity on the branch cut at $u = 0$. Formal integration can be performed by Cauchy residue theory. Evaluation of the $u = -x_1$ residue in view of eqn (18) and substituting it into the right-hand side of eqn (19) gives a result which is identical in form to the negative of T_{2b} when $x_2 = 0$. Evaluation of the residues of the other simple poles, and substitution of them into the right-hand side of eqn (19) gives

$$\frac{\mu b}{2\pi\sqrt{(x_1 - C_1)}} \int_{s_0}^{t^*} \dot{D} \frac{\partial}{\partial \phi} \mathrm{Im} \frac{\sqrt{z_1}}{Z z_0} \mathrm{e}^{\mathrm{i}(\phi - \beta)} \mathrm{d}t, \qquad z_k = r_k \mathrm{e}^{\mathrm{i}\omega_k}, \qquad Z = X \mathrm{e}^{\mathrm{i}\Theta} \tag{23}$$

$$X_1 - x_1 = r_0 \cos\omega_0, \qquad X_2 = r_0 \sin\omega_0. \tag{24}$$

The parameters (r_0, ω_0) are the polar coordinates of the trajectory points $\mathbf{X}$ at $S = D(t)$ with respect to the point $(x_1, 0)$. Study of the ϕ-derivative in eqn (23) in view of Fig. 1(b) shows that it is identical to

$$-\frac{\partial}{\partial S} \mathrm{Re} \frac{\sqrt{z_1}}{z_0}. \tag{25}$$

Therefore, introducing the variable change $S = D(t)$ and recognizing that $D(s_0) = 0$ allows eqn (23) to be integrated exactly. Combining the result with the $u = x_1$ residue term in eqn (19) then gives

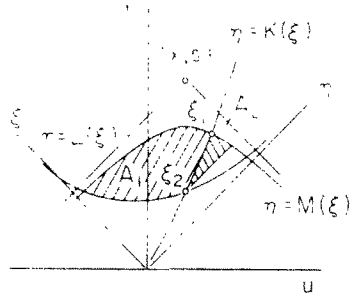

Fig. 2. Integration region in the u–t plane.

$$T_{2c} = -T_{2b} + \frac{\mu b}{2\pi\sqrt{(x_1 - C_1)}} \operatorname{Re}\left[\left(\frac{\sqrt{z_1}}{z_0}\right)^0 - \left(\frac{\sqrt{z_1}}{z_0}\right)^*\right] \tag{26}$$

for $x_2 = 0$, $C < x_1 < s$, where x_1 is small. Here $(\,)^0$ denotes a quantity evaluated at $t = s_0$, $(S, N) = 0$.

6. SIMPLIFICATION OF w_c

With eqn (26) available, eqn (11) for the case w_c can now be simplified. Figure 2 shows a schematic of the integration area A in the u–t plane, when x lies within the region corresponding to the interior of the cylindrical shear wave generated by the dislocation signal diffraction. Equation (6a) defines T_{2c} in the portion designated as A_1, while eqn (26) is valid in the portion A_2. Since the term $-T_{2b}$ appears in both equations, i.e. everywhere in A, its contribution to the right-hand side of eqn (11) involves w_b. The more interesting contribution to w_c, therefore, is in the second term in eqn (26).

By redefining the characteristic variables (ξ, η) in terms of the integration variables (u, t), it is easily shown in view of Fig. 2 that both contributions of the second term in eqn (26) to the right-hand side of eqn (11) have the form

$$\frac{b\sqrt{r_1}}{2\pi^2\mu}\int_{\xi_2}^{\xi_1}\int_K^M \frac{1}{r_0}\cos\left(\frac{\omega_1}{2} - \omega_0\right)\frac{d\eta}{\sqrt{(M-\eta)}\sqrt{(\eta - K)}}\frac{d\xi}{\sqrt{(s - x_1 - \sqrt{2}\xi)}} \tag{27}$$

where $M(\xi)$ and t^* are now given by

$$\sqrt{2}M = \frac{s^2 - x^2 - \sqrt{2}\xi(s + x_1)}{s - x_1 - \sqrt{2}\xi}, \qquad t^* = \sqrt{2}\xi + C_1 - r_1^*, \qquad x = |\mathbf{x}| \tag{28}$$

while (ξ_1, ξ_2) can be obtained by solving, respectively, the relations

$$M = K, \qquad L = K \tag{29a, b}$$

for ξ. It is readily shown that the (r_0, ω_0)-dependent term in eqn (27) can be written as

$$\frac{1}{(\eta - \xi - \sqrt{2}X_1)^2 + 2X_2^2}\left[(\sqrt{2}X_1 + \eta - \xi)\cos\frac{\omega_1}{2} + \sqrt{2}X_2\sin\frac{\omega_1}{2}\right]. \tag{30}$$

The η-integration in eqn (27) is now recognized as an integration along the branch cut $K < \eta < M$ of an integrand which exhibits simple poles at $\eta = \xi + \sqrt{2}X_1 \pm i\sqrt{2}|X_2|$. Formal integration can be performed by means of Cauchy residue theory. Evaluation of these residues and substitution into the ξ-integral gives a complicated expression. This

can, however, be simplified by reintroducing u as an integration variable through the substitution $s - \sqrt{2}\xi = u$, and by defining the parameters (r_2, ω_2) and (r_3, ω_3) as follows:

$$X_1 - C_2 = r_2 \cos\omega_2, \qquad X_2 = r_2 \sin\omega_2, \qquad C_2 = C(s_2) \tag{31}$$

$$2(u - x_1)X_1 + x^2 - u^2 = r_3 \cos\omega_3, \qquad 2(u - x_1)X_2 = r_3 \sin\omega_3. \tag{32}$$

The result is that the contribution of the second term in eqn (26) to w_c can be written as

$$\frac{b}{2\pi}\mathrm{Re}\left[z_1^0 \int_{u_1}^{u_2} \frac{du}{\sqrt{(z_2 z_3)^0}} - \int_{u_1}^{u_2} \frac{\sqrt{z_1^*}\,du}{\sqrt{(z_2 z_3)^*}}\right]. \tag{33}$$

Here (r_2, ω_2) are the polar coordinates of trajectory points $\mathbf{X}$ with respect to the point $\mathbf{x} = (C_2, 0)$ and the instants (s_2, t^*) are now defined by

$$s_2 - C_2 = s - u, \qquad t^* = s - u + C_1 - r_1^*. \tag{34}$$

In view of eqns (15), (21) and (28), (u_1, u_2) can be derived from the relations

$$\tau_1 = s - x_1 - \frac{x_2^2}{s + x_1 - \sqrt{2}K\left(\dfrac{\tau_1}{\sqrt{2}}\right)}, \qquad \tau_2 = s_0 - d_1 - \frac{d_2^2}{s_0 + d_1 - \sqrt{2}K\left(\dfrac{\tau_2}{\sqrt{2}}\right)} \tag{35}$$

where $\tau_k = s - u_k$ and it can be shown that $s_1 > s_2$.

7. SIMPLIFICATION OF T_{2c}^0, w_c^0

Similar approximate integration schemes can be applied to eqns (11) and (13) and, indeed, are simpler owing to the less complicated form of T_2^0. The results are that for $x_2 = 0$, $C < x_1 < s$, x_1 small

$$T_{2c}^0 = -T_2^0 - \frac{\mu b}{2\pi\sqrt{(x_1 - C_1)}}\mathrm{Re}\left(\frac{\sqrt{z_1}}{z_0}\right)^0 \tag{36}$$

where from eqns (10) and (4a), we find that along $x_2 = 0$

$$T_2^0 = -\frac{\mu b}{2\pi}\sqrt{\left(\frac{d}{x_1}\right)}\frac{(d - x_1)\cos\dfrac{\psi}{2}}{(d_1 - x_1)^2 + d_2^2} \tag{37}$$

for $x_1 > 0$ and vanishes otherwise. Similarly, for all $x < s$, the contribution of the second term in eqn (36) to w_c^0 is

$$-\frac{b}{2\pi}\mathrm{Re}\sqrt{z_1^0}\int_{u_1}^{s} \frac{du}{\sqrt{(z_2 z_3)^0}}. \tag{38}$$

With eqns (36)–(38) at hand, the solution to the basic problem described by eqns (1)–(3) is complete, while its validity, strictly speaking, is confined to the vicinity of the initial crack edge, the solution contains the fully transient nature which would result from exact integrations of eqns (12) and (13). The situation to which this solution will be applied is discussed in the next section.

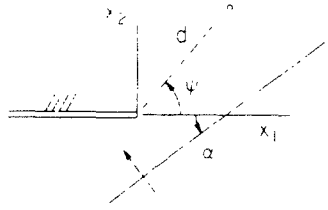

Fig. 3. SH-wave incident upon crack edge.

8. A DIFFRACTION PROBLEM APPLICATION

It is well known, e.g. Ref. [13], that, due to the dynamic overshoot phenomenon, the diffraction of stress waves by a crack edge is an important source of dynamic brittle fracture. We, therefore, now consider the problem illustrated in Fig. 3: a plane SH-wave of uniform stress T_0 impinges upon the same crack–dislocation combination considered in the basic problem, and reaches the crack edge at $s = 0$. The out-of-plane displacement generated by the wave is

$$w_i^0 = T_0(s + x_1 \sin\alpha - x_2 \cos\alpha) \tag{39}$$

where α is the wavefront angle made with the crack plane. If the dislocation were not present, then the problem would reduce to one of crack propagation initiated at $s = 0$ by wave diffraction. The solution to this type of problem has been studied[12], and can be written as $w_1 + w_i^0$, where $w_i(\mathbf{x}, s)$ is given by eqns (11) and (12), with T_{2b} replaced by T_{2i} and the lower integration limit L replaced by $-\kappa\xi$, where

$$\kappa = \frac{1 - \sin\alpha}{1 + \sin\alpha}. \tag{40}$$

These formal relations can be simplified in a manner similar to that employed above, with the exact result that

$$T_{2i} = -T_{2i}^0 - \frac{2}{\pi} T_0 \cos\alpha \left(\frac{1}{\sqrt{P}} + \tan^{-1}\sqrt{P} \right), \quad P = \frac{x_1 - C_1}{C_1 + \frac{1}{2}(1 + \kappa)(s - x_1)} \tag{41}$$

for $x_2 = 0$, $C < x_1 < s$, where

$$T_{2i}^0 = -T_0 \cos\alpha \tag{42}$$

while the equation corresponding to eqn (33) is

$$-\frac{1}{\pi} T_0 \cos\alpha \int_{u_1}^{s} \sqrt{[(u - x_1)(s + x_1 + \kappa(s - u)) - x_2^2]} \frac{du}{u - x_1} \tag{43}$$

where (u_1, C_1) are again defined by eqns (35), (20) and (21). Equations (1)–(3) show clearly that the solution for the complete problem shown in Fig. 3 is simply $w^0 + w_i^0 (s < 0)$ and $w + w_i^0 + w_1 (s > 0)$.

The dislocation motion is as yet largely arbitrary, so for purposes of illustration, we now impose the following behavior: The dislocation starts to move when the cylindrical rotational wave generated at the crack edge at $s = 0$ arrives, it subsequently follows a

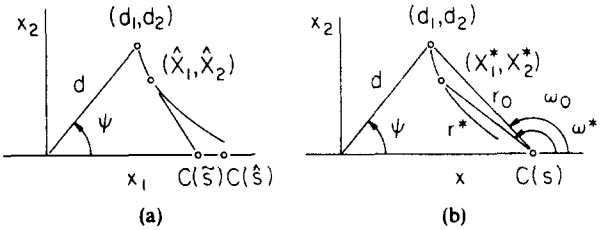

Fig. 4. (a) Dislocation position as defined by crack edge position. (b) Parameters for dynamic stress intensity factor.

trajectory Γ such that its velocity is always directed toward the crack edge, and stops if it reaches the crack edge. That is

$$s_0 = d \tag{44}$$

and, as Fig. 4(a) shows, the dislocation trajectory tangent passes through the instantaneous crack edge position. Moreover, the sign of ψ determines the sign of X_2.

Assumption of this motion is based on the quasi-static result[5] that the force on the dislocation in a cracked but otherwise undisturbed unbounded medium is a maximum along the straight line between the dislocation and the crack edge. In a dynamic analysis, of course, there is a delay due to signal travel time, so that, as Fig. 4(a) indicates, the dislocation position $\mathbf{X}$ at $s = \hat{s}$ is defined by the crack edge at $s = \tilde{s} < \hat{s}$. It can be shown that the differential equation for Γ is

$$\frac{X_2 X_2''}{X_2'^2\sqrt{(1 + X_2'^2)}} = \pm\lambda, \qquad \lambda = \frac{dC}{dD} \tag{45a,b}$$

where $X_2 = X_2(X_1)$ and $\pm$ denotes the sign of $-X_2'/X_2$. We here take $(\dot{C}, \dot{D})$ as the constants $(\dot{C}_0, \dot{D}_0)$, and eqn (45a) is then readily integrated for the case $\lambda \neq 1$ to yield the equation pair

$$2\dot{D}_0(s - d) - \left(\frac{d - \lambda d_1}{1 - \lambda^2}\right) + \left(\frac{d + d_1}{1 - \lambda}\right)y^{1+\lambda} + \left(\frac{d - d_1}{1 - \lambda}\right)y^{1-\lambda} = 0, \qquad y = \frac{X_2}{d_2} \tag{46a,b}$$

$$X_1 + \dot{D}_0(s - d) = \left(\frac{d - \lambda d_1}{1 - \lambda^2}\right) - \left(\frac{d - d_1}{1 - \lambda}\right)y^{1-\lambda}. \tag{46c}$$

For a given s, eqn (46a) is solved for X_2, whereupon eqn (46c) yields X_1. For $\lambda = 1$ the results are

$$2\dot{D}_0(s - d) + (d - d_1)\ln y + \frac{1}{2}(d + d_1)(y^2 - 1) = 0 \tag{47a}$$

$$X_1 + \dot{D}_0(s - d) = d_1 - (d - d_1)\ln y. \tag{47b}$$

Equations (46) and (47) can be used to show that the dislocation never reaches the crack surface when $\lambda \geqslant 1$. For $\lambda < 1$ however, contact occurs at $X_1 = X_L$ when $s = s_L$, where

$$s_L = \frac{d}{1 - \dot{C}_0} + \frac{1}{\dot{D}_0}\left(\frac{d - \lambda d_1}{1 - \lambda^2}\right), \qquad X_L = \lambda\left(\frac{d - \lambda d_1}{1 - \lambda^2}\right). \tag{48}$$

These results are employed in the next section to study the dynamic stress intensity factor.

9. DYNAMIC STRESS INTENSITY FACTOR

We define the dynamic stress intensity factor K_2 as

$$K_2 = \lim_{x_1 \to C^+} \sqrt{(x_1 - C_1)} T_2(x_1, 0, s). \tag{49}$$

Based on this definition, eqns (26), (36), (37), (41) and a limit process discussed in Ref. [12] it is readily shown that when $\lambda \geqslant 1$

$$s < 0: \qquad \frac{1}{\mu\sqrt{R_0}} K_2 = k_b(d, \psi, 0) \tag{50a}$$

$$0 < s \leqslant s_c: \qquad \frac{1}{\mu\sqrt{R_0}} K_2 = k_i - k_b(r_0, \omega_0, \dot{C}_0), \qquad s_c = 2\left(\frac{d - \dot{C}_0 d_1}{1 - \dot{C}_0^2}\right) \tag{50b,c}$$

$$s \geqslant s_c: \qquad \frac{1}{\mu\sqrt{R_0}} K_2 = k_i - k_b(r^*, \omega^*, \dot{C}_0) \tag{50d}$$

where

$$k_i = \frac{2}{\pi} \frac{T_0}{\mu} \sqrt{(1 - \dot{C}_0)} \sqrt{\left(\frac{s}{R_0}\right)} \cos\alpha, \qquad k_b(r, \omega, v) = \frac{1}{2\pi} \frac{b}{R_0} \sqrt{\left(\frac{R_0}{r}\right)} \sqrt{(1 - v)} \cos\frac{\omega}{2} \tag{51}$$

and R_0 is any microstructural characteristic length. As Fig. 4(b) shows, $(r, \omega)_0$ and $(r, \omega)^*$ are the polar coordinates of, respectively, the initial dislocation position and the dislocation position at $s = s^*$ with respect to the crack edge. The equation

$$s^* = s - \sqrt{[(X_1^* - \dot{C}_0 s)^2 + X_2^{*2}]} \tag{52}$$

indicates that a signal must leave the dislocation at s^* in order to arrive at the crack edge at s. Finally, s_c is the instant that the crack edge is first aware of the dislocation. For $\lambda < 1$, these results must be modified by recognizing that eqn (50d) holds only for $s_c \leqslant s \leqslant s_L$. For $s \geqslant s_L$

$$\frac{1}{\mu\sqrt{R_0}} K_2 = k_i. \tag{53}$$

In words, eqns (50)–(53) can be explained as follows: for $s < 0$ the equilibrium dislocation governs K_2, but for $0 < s \leqslant s_c$, K_2 has two components, k_i due to the SH-wave diffraction and k_b due to the removal of the equilibrium dislocation stress field by the propagating crack. For $s \geqslant s_c$, k_b is now due to the removal of the moving dislocation stress field. In addition, when $s \geqslant s_L$ for $\lambda > 1$, K_2 is governed only by the SH-wave diffraction. It is also noted that, in general, K_2 behaves continuously except at crack propagation initiation ($s = 0$).

10. DYNAMIC STRESS INTENSITY FACTOR FOR A DISLOCATION ARRAY

To generalize the expressions for K_2 to an n-member array, one need only treat the parameters $(d, \psi, b, \dot{D}_0)$ as array variables, and sum k_b with respect to them. To illustrate such an array, we consider two cases.

(1) The dislocations are arrayed around the circumference of a circle of radius R_0 centered at the initial crack edge, i.e. $d/R_0 = 1$, $|\psi| < \pi$.

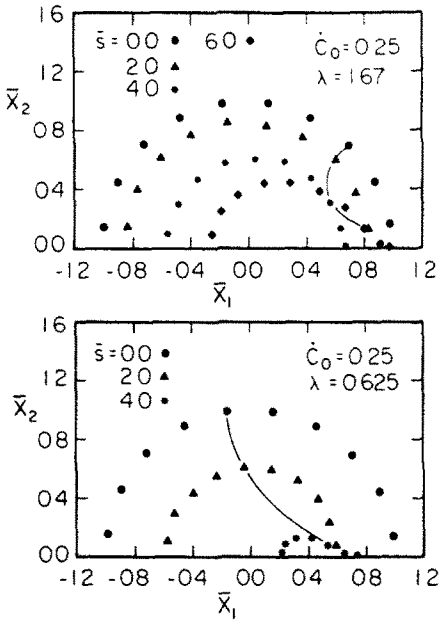

Fig. 5. Dislocation trajectories for case (1).

(2) The dislocations are arrayed around the same circle, except that its center is now a distance R_0 ahead of the initial crack edge, i.e. $d/R_0 = 2\cos\psi$, $|\psi| < \pi/2$.

In both cases, the dislocations are evenly spaced around the circles, are distributed symmetrically with respect to the x_1-axis, and move with the same speed $\dot{D}_0$.

In Fig. 5, the motion of the dislocations when $\psi > 0$ for case (1) is illustrated when $n = 20$, $\dot{C}_0 = 0.25$ and either $\lambda = 1.67$ or 0.625, where $\bar{()}$ denotes nondimensionalization with respect to R_0. The curves in Fig. 5 are examples of dislocation trajectories, but dislocations which have reached the crack surface are deleted. Corresponding motions for case (2) are given in Fig. 6.

Both figures show that, as should be expected, the dislocation arrays form a band near the crack surface, and eventually collapse onto it if $\lambda < 1$. These results agree with observations of inelastic zone shapes after crack propagation has ceased[1].

To show the effect of dislocation arrays on the dynamic stress intensity factor, we consider again cases (1) and (2), but with $n = 38$ and the physically reasonable dimensionless parameter values

$$\frac{1}{\mu}\left|T_0\right| = 0.0001, \qquad \left|\frac{b}{R_0}\right| = 2.5(10^{-7}), \qquad \alpha = 0 \tag{54}$$

chosen. In Fig. 7, the SH-wave diffraction contribution k_i is plotted vs $\bar{s}$, along with the envelopes of K_2 itself for cases (1) and (2), where $\lambda = 1.67$ and 0.625. It is seen that the dislocation arrays have a noticeable effect on K_2, either intensifying or relaxing it in accordance with the sign of b/T_0. It is also seen, however, that the effect dies out in little more than the rotational wave travel time from the initial crack edge position to the initial dislocation array periphery.

11. SUMMARY

This article considered dislocation–crack edge interaction in inelastic zones formed near the edges of propagating cracks during dynamic brittle fracture. In particular, it presented the exact transient solution of a screw dislocation moving near the edge of a

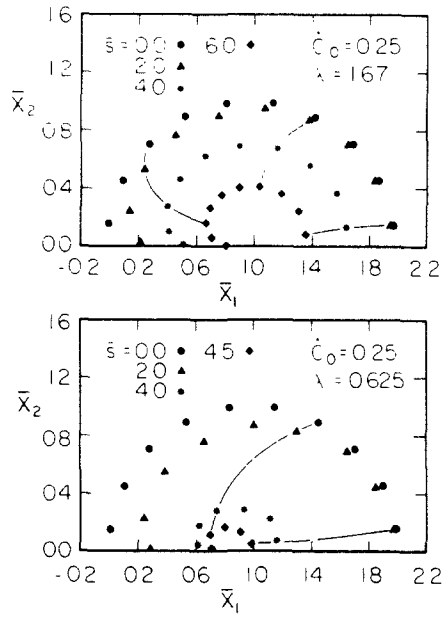

Fig. 6. Dislocation trajectories for case (2).

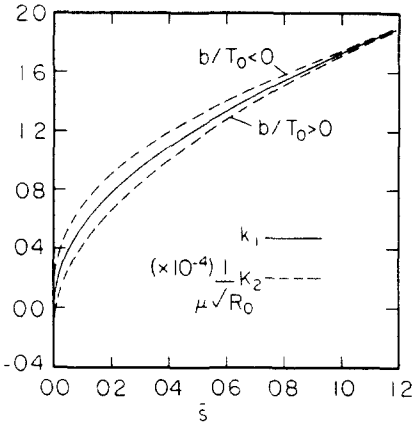

Fig. 7. Dynamics stress intensity factor response.

propagating Mode III crack, and applied it to a problem of screw dislocation arrays and a crack whose propagation is triggered by plane SH-wave diffraction.

Under a simple law based on a dislocation force concept, it was shown in light of this problem that, if the dislocations move at speeds greater than the crack edge, they eventually reach the crack surface and cease to affect the dynamic stress intensity factor. Otherwise, the dislocations only approach the crack surface asymptotically. The resultant array configurations in both cases appear to agree with inelastic zone shapes noted near arrested cracks. It was also shown that the arrays have a noticeable if brief effect on the dynamic stress intensity factor.

The results of this article were preliminary in scope. Future efforts will consider experimentaly observed dislocation densities and inelastic zone shapes. In addition, the present results accounted only for those dislocations existing initially around the crack edge, and assumed that their motion was independent of the original slip planes. Future efforts will consider the new inelastic zone area which is generated during crack propagation. Finally, the criteria for fracture initiation and crack propagation will be considered. All these efforts, however, will be based on the expressions presented here.

Acknowledgement—This research was supported by NSF Grant MEA8319605 to LMB, and was performed while LMB was a 1985 Navy/ASEE Summer Faculty Research Associate at the Naval Research Laboratory in Washington, DC.

REFERENCES

1. H. L. Ewalds and R. J. H. Wanhill, *Fracture Mechanics*. Edward Arnold, Baltimore (1984).
2. G. I. Taylor, The mechanism of plastic deformation of crystals. *Proc. R. Soc. London* **A145**, 362–415 (1934).
3. K. Jagannadham and M. J. Marcinkowski, *United Theory of Fracture*. Trans Tech Publications, Rockport, Massachusetts (1984).
4. E. W. Hart, A theory for stable crack extension rates in ductile materials. *Int. J. Solids Structures* **16**, 807–823 (1980).
5. B. S. Majumdar and S. J. Burns, An elastic theory of dislocations, dislocation arrays and inclusions near a sharp crack. *Acta Metall.* **29**, 579–588 (1981).
6. R. M. Thomson and J. E. Sinclair, Mechanics of cracks screened by dislocations. *Acta Metall.* **30**, 1325–1334 (1982).
7. L. M. Brock, The dynamic stress intensity factor for a crack due to arbitrary rectilinear screw dislocation motion. *J. Elasticity* **13**, 429–439 (1983).
8. L. M. Brock, The dynamic stress intensity factor due to arbitrary screw dislocation motion. *ASME J. Appl. Mech.* **50**, 383–389 (1983).
9. L. M. Brock, Transient dynamic Green's functions for a cracked plane. *Q. Appl. Math.* **44**, 265–275 (1986).
10. R. Burridge and L. Knopoff. Body force equivalents for seismic dislocations. *Bull. Seism. Soc. Am.* **54**, 1875–1888 (1964).
11. L. M. Brock, Transient solution for arbitrary growth of screw dislocation distributions near a crack, University of Kentucky College of Engineering Technical Report (November 1985).
12. J. D. Achenbach, Extension of a crack by a shear wave. *Z. Angew. Math. Phys.* **21**, 887–900 (1970).
13. L. M. Brock, Quasi-sudden brittle fracture at both edges of a finite crack. *Int. J. Engng Sci.* **12**, 553–568 (1974).